Fuzzy rule-based model for contaminant transport in a natural river channel

Helen Kettle, Barry Hankin and Keith Beven

ABSTRACT

Fuzzy rules are used to model solute dispersion in a river dead zone, such that the turbulent diffusion is determined by a fuzzy inference system which relates the local mean velocity shear to the longitudinal velocity fluctuations. A finite-volume hybrid scheme is applied to a non-orthogonal grid for which a mean velocity field is produced using the computational fluid dynamics (CFD) package Telemac 2D. At each cell face fuzzy rules predict a fuzzy number, and these numbers reflect the possible magnitudes of turbulent velocity fluctuations. These are input to the finite-volume model using a single-value simulation method. Multiple model runs produce a fuzzy number for the solute concentration in each cell. The results of the fuzzy model are then compared with data collected in a field experiment with rhodamine dye in the River Severn.

Key words | contaminant transport, dead zone, fuzzy, solute dispersion

Helen Kettle (corresponding author)
Department of Geology and Geophysics,
University of Edinburgh,
Kings Buildings,
Edinburgh EH9 3JW,
Scotland,
UK
Tel: (+44) 0131 650 8511
E-mail: *Helen.Kettle@glg.ed.ac.uk*

Barry Hankin
Keith Beven
Environmental Science,
Lancaster University,
Lancaster LA1 4YQ,
UK
Tel: (+44) 01524 593975
Fax: (+44) 01524 593985
E-mail: *b.hankin@lancaster.ac.uk*
Tel: (+44) 01524 593892
Fax: (+44) 01524 593985
E-mail: *K.Beven@lancaster.ac.uk*

INTRODUCTION

The transport and mixing of a solute as it travels downstream in a natural channel is affected to a large extent by the geometry of the river through which it travels. In particular, areas of slow-moving, recirculating or stagnant water in the regions near the banks, often known as 'dead zones', are thought to trap and retain tracer dyes, thus creating a long tail in the tracer curve further downstream. Owing to the relatively slow movement of water in the dead zone, a shear zone is created between it and the main flow, and thus the dead zone will often act as a distinct cell which is separate from the main flow. Exchanges of momentum and transported scalar properties, such as heat and solute concentration, between these two regions occur at variable rates across the shear zone. It is therefore important that the exchanges that take place in these dead zone regions are well understood.

To gain further insights into the processes at work in the dead zone region, a numerical model has been developed. There are many computational fluid dynamics (CFD) packages available to model mass transport but in general these rely on the theory of Fickian turbulent diffusion, whereby a turbulent diffusion coefficient, analogous to molecular diffusion, is thought to exist (Taylor 1921). The turbulent diffusion coefficient is notoriously hard to estimate for natural channels (Young & Wallis 1993), and therefore a different technique has been suggested based on fuzzy rules. The fuzzy dispersion model developed here relies on the hypothesis that the turbulent diffusion fluxes of a scalar property are a direct result of the turbulent velocity fluctuations. This supposition is supported by previous work in a laboratory flume (Kettle & Beven 2001). The fuzzy model allows the uncertainties in our knowledge of the turbulent field to be incorporated directly into the model. These uncertainties are then carried through the model to produce a distribution of possible tracer fields resulting from the different possible fluctuating fields.

However, in order to model the dispersion of the tracer, the mean velocity field must be known. This is calculated using the CFD package Telemac 2D, in which a semi-distributed constant-eddy viscosity model is employed. The flow domain is divided into three different

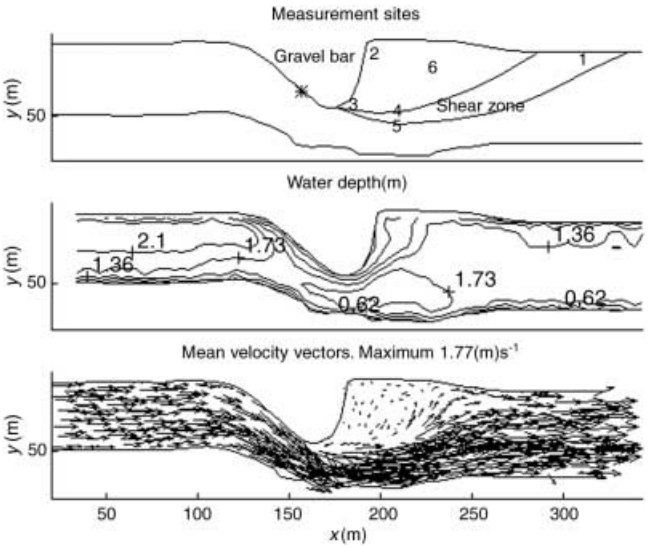

Figure 1 | Site of experiment with numbered measurement points marked, depth of river bed, and mean velocity field produced by TELEMAC-2D. Dye injection point is shown by an asterisk in the first plot. The third plot depicts only a selection of the velocity vectors from the grid used in the model to allow greater clarity.

zones: the dead zone, the main flow and a shear zone that separates them. This was justified on the basis of local transverse components of Reynold's stresses calculated from acoustic Doppler velocimeter (ADV) measurements of turbulent time series within the different zones. These stresses, which can be interpreted as turbulent fluxes of momentum, were found to vary considerably, with values of 0.479, 2.053 and 0.09 kg m^{-1} s^{-2} in the main flow, shear zone and dead zone, respectively. Multiple runs of Telemac 2D were used to find the parameter sets which gave stable flow fields that approximately satisfied the constraints introduced by the velocity data observed (see Hankin *et al.* 2001). The appropriate parameters were found to be an eddy viscosity of 0.03 kg m^{-1} s^{-1} and Manning's n of 0.045 in the dead zone, an eddy viscosity of 0.018 kg m^{-1} s^{-1} and $n = 0.025$ in the shear zone, and an eddy viscosity of 0.027 kg m^{-1} s^{-1} and $n = 0.039$ in the main channel. The results of this simulation are shown in Figure 1. The mean velocity field used in the mixing model is not an exact match with the field velocity measurements since Telemac 2D slightly underestimates the longitudinal and lateral extent of the dead-zone region into the main flow. However, if observed and predicted velocities are compared at locations relative to the shear zone they show reasonable agreement, implying that the mean flow field is of the correct order of magnitude. Given the uncertainty involved in taking field velocity measurements, as well as in the conversion of a fully three-dimensional system to two dimensions, the velocity field was accepted as adequate.

The fluctuating velocity field is calculated using the transverse velocity shear in a set of fuzzy rules derived from flume data described in Kettle & Beven (2001). Once a fuzzy number for the longitudinal velocity fluctuation u' (the root mean square of the temporal deviations from the mean longitudinal velocity) has been calculated, a single value of u' is chosen at random. This is then used to find a corresponding fuzzy number for the cross-stream velocity fluctuation v', from which a single value is chosen. The model is run in this way using several hundred realizations, each with a slightly different fluctuating field, to produce a fuzzy number for the solute concentration in each cell. This approach attempts to capture some of the uncertainty inherent in the system, and to carry this through the model without loss of information.

METHODS

Experimental equipment and procedures

Dead-zone site

The chosen reach is on the River Severn at Leighton, which is close to Shrewsbury in Shropshire. In this region the river is up to 80 m wide, with a classic meandering sequence with alternating gravel point bars and steeply cut banks. The dead zone under investigation lies immediately downstream of a gravel bar, as shown in Figure 1. The dead zone contains slow-moving recirculating water that is separated from the main flow by a visibly turbulent shear-zone region.

Velocity measurements

Velocity measurements were taken using an acoustic Doppler velocimeter (ADV) that measures instantaneous

flow velocities in three dimensions. The ADV samples are taken at 25 Hz, over a measuring volume of approximately 1 cc, located 5 cm below the sensor head. The accuracy of this instrument was investigated by Lane *et al.* (1998) and was found to give good results for mean flow velocities. Velocity measurements were taken at the tracer sites at a depth which allowed submersion of the probe, and vertical velocity profiles were measured at intervals across the width of the main flow, upstream of the dead zone, using an Ott electromagnetic current meter array. These measurements were depth-averaged and used as input for the velocity field simulation in Telemac 2D.

Tracer measurements

The rhodamine tracer was released at a steady rate for 220 min into the main flow upstream of the dead zone. Water samples were then taken from the river at six strategic sites (see Figure 1).

SITE 1. This location marks the 'reattachment zone', i.e. the point where fluid from the main flow enters the recirculation zone by advection.

SITE 2. This site is at the furthest end of the dead zone, and samples from here should be from water that has travelled almost completely through the dead zone.

SITE 3. This site marks the beginning of the shear zone, where fast-moving water meets the slowing, recirculating dead-zone water.

SITES 4 and 5. These sites lie either side of the shear zone, and give an insight into how the flow structure affects dispersion.

SITE 6. This site is approximately in the centre of the dead zone.

Ten minutes after release of the dye, discrete bottled samples were collected simultaneously at Sites 1–5. Thereafter, samples were collected at 15-min intervals. Site 6 was sampled every 2 s using an *in situ* fluorometer. Samples were taken at approximately 0.5 m below the water surface, or at half the water depth in very shallow sites. The dye pump was switched off after 220 min, but the manual sampling continued until 345 min after the release, and the fluorometer continued to sample for a further 163 min, after which time the concentration levels in the dead zone had returned to the background level.

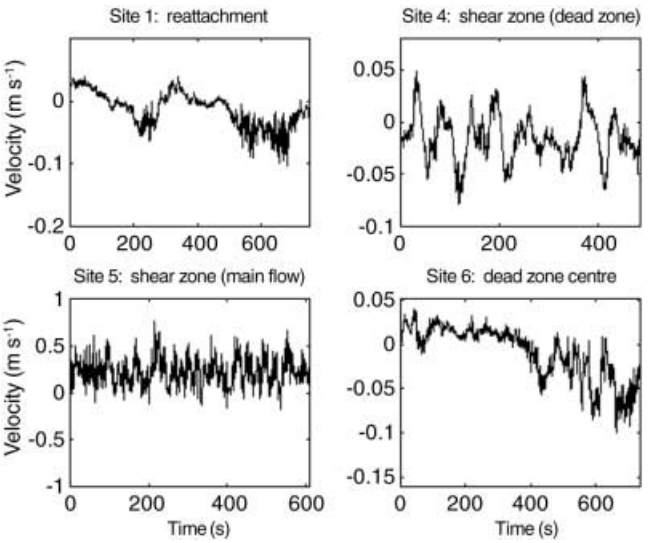

Figure 2 | Time series data for mean longitudinal velocity, *U*, at 4 tracer sites.

Velocity and turbulence characteristics

Figure 2 shows the time-series data for the longitudinal velocity, *U*, which is taken to be in the *x* direction on the axes in Figure 1. The plots clearly show that each of the sites is affected by periodic forcing of differing frequencies. Using a Fourier transform, the dominant time period was calculated. The reattachment site (Site 1) shows the strongest periodicity, with a time period of 375.5 s. However, the time-series plot indicates that there exists another much larger time period, but the data were not collected for long enough to capture this. It is thought that this longer period may be associated with recirculation in the dead zone, which also appears to cause a periodic lateral movement of the shear zone, as was observed in the field. The dead-zone side of the shear zone (Site 4) has a time period of 60.8 s, whilst the main flow side of the shear zone (Site 5) has a time period of 67.8 s and the data do not indicate a larger periodicity is present. The site of the fluorometer (Site 6) near the centre of the dead zone has a time period of 246.3 s along with a much larger time period on a similar time scale to that in the reattachment zone. Again, the time series does not continue for long enough to capture this. Thus, it can be seen that the dead zone exhibits a complex time-dependent flow structure. However, for modelling purposes it is simpler to assume a

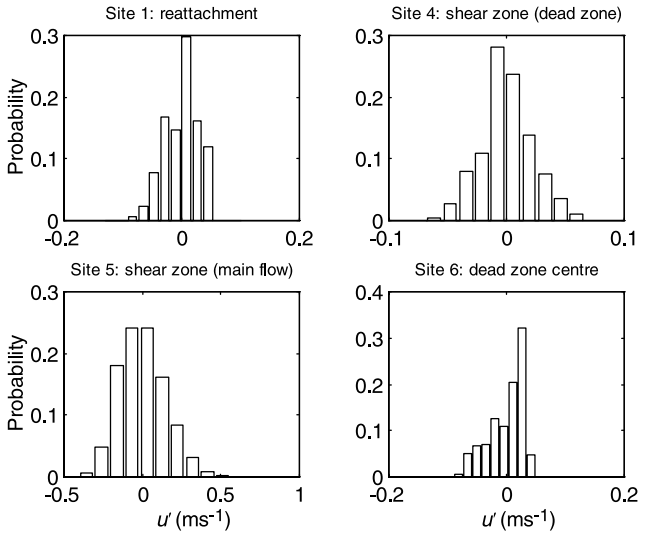

Figure 3 | Probability distributions for u'.

steady flow. Therefore the flow is considered to be steady, such that the mean velocity is taken from the time series, and the root mean square of the deviations from this mean are represented in the fluctuating velocity u'. Figure 3 shows the probability distributions of the temporal fluctuations from the mean velocity. These are calculated by dividing the range between the minimum and maximum recorded velocities in each time series into ten equal intervals and summing up the number of values in each interval. However, these distributions are biased according to which section of the dominant time period the velocity data were collected in. To approach a non-skewed distribution, the data must be collected over a time period that is a multiple of the lowest-frequency periodic motion. Sites with a smaller time period show symmetrical distributions, whereas the reattachment zone and the fluorometer site show negatively skewed distributions.

If only the means of the time series data are considered, the sites may be summarized as shown in Table 1. This table shows that the mean velocity varies by an order of magnitude over the shear zone. This is reasonable, since the dead-zone water is in the lee of the gravel bar and is hardly affected by the main flow expect by the diffusion of momentum across the shear zone and a gentle recirculation generated when the main flow hits the bank at the far end. At this point, the fast-moving water has spread out to both banks and has lost some of the high speed it reached at the constriction point at the start of the gravel bar.

Tracer results

Bottled samples were analysed in the laboratory with the calculated concentrations standardized to a temperature of 20°C. Figure 4 shows the changes in tracer concentration at each site. Site 3 has been inserted separately because the concentration is an order of magnitude greater than that at the other sites. The dye first appears at Site 5 (main flow) and then reaches Site 1 (the reattachment zone). The dye then appears at Site 4 (the dead zone side of the shear zone). It may have reached here by turbulent diffusion through the shear zone, or by catching a fast zone of recirculation in the dead zone. After 30 min from the release time, the tracer reaches the centre of the dead zone (Site 6). However, it is not until 100 min after

Table 1 | Velocity characteristics of four tracer sites. All velocities are in cm s^{-1}

Site	Description	U	V	W	u'	v'	w'
1	Reattachment	– 1.35	0.20	0.061	2.81	1.67	0.85
4	Shear zone (dead zone)	– 1.54	– 3.87	– 0.48	2.2	2.18	0.88
5	Shear zone (main flow)	22.3	– 44.53	– 1.72	14.42	12.13	7.86
6	Centre of dead zone	– 0.95	– 2.51	– 0.32	2.96	1.6	0.92

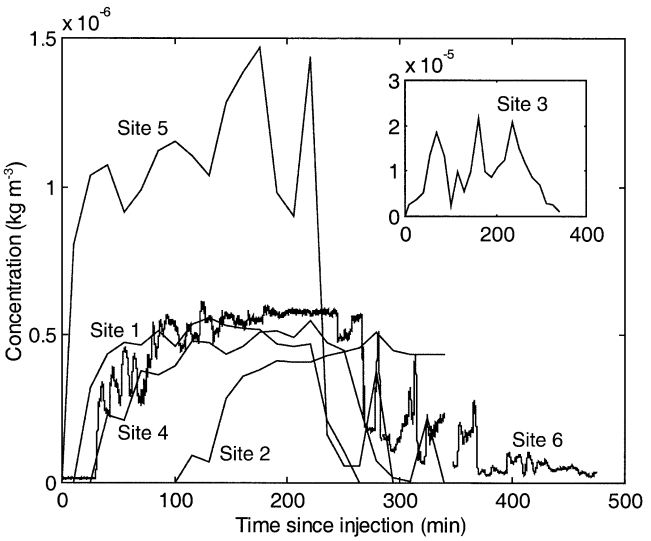

Figure 4 | Tracer time curves at each site.

the release time that the tracer reaches the far side of the dead zone (Site 2). The tracer is recorded at Site 3 as soon as the dye is released, and shows very large fluctuations in concentration over the time period monitored. This is probably because the site is in a shallow area near the bank that may itself be a miniature dead zone which is periodically flushed by the large-scale lateral movement of the shear zone.

Fuzzy sets and fuzzy rules

A *fuzzy set* is a set of objects in which each object has a *membership function* assigned to it that indicates the extent to which the object belongs to the set. An example of a fuzzy set is the set of 'fast velocities'. Since there is no definite boundary between 'fast' and 'not fast', each velocity reading belongs to the set to a different degree. The membership function of fuzzy set A is denoted by μ_A, and is a mapping from the universal set, X, to the interval of real numbers from 0 to 1 inclusive. The closer that $\mu_A(X)$ is to 1 the more X belongs to A, and the closer it is to 0 the less it belongs to A.

Each fuzzy rule used in this work contains only input and one output, so that logical operators (e.g. AND and OR) are not incorporated. In Boolean logic, a rule can either apply with absolute certainty or not apply. In fuzzy logic, a rule may partially apply, so that there may be cases where a few different rules with different consequences can, to a certain degree, be applied to the same input. The level to which a rule applies to a given input is termed the degree of fulfilment (DOF) of a fuzzy rule and is a value in the interval [0,1]. Figure 4 shows how two rules may be used by one input, and how the consequence of each rule may be combined to produce the final output fuzzy set. There are many methods for combining the rule responses (see Dubois & Prade 1991; Bardossy & Duckstein 1995); in this work the sum method is used, in which the final output is simply the sum of all fuzzy sets given by the rules.

Fuzzy rules for u'

The fuzzy rules used to predict the fluctuating field were derived from velocity data collected in a laboratory flume (see Kettle & Beven 2001). From these data, a set of non-dimensional rules was developed relating the transverse velocity shear $|\partial U/\partial y|/(U_f/h)$ to the mean longitudinal velocity fluctuation u'/U_f, where h is the mean water depth and U_f is the mean channel velocity. The fuzzy inference system consists of one input ($|\partial U/\partial y|/U_f/h$) and one output ($u'/U_f$), as shown in Figure 5. Both have five membership functions and the system is described by the five rules:

1. *If* $|\partial U/\partial y|/(U_f/h)$ *is in fuzzy set 1, then* (u'/U_f) *is in fuzzy set 1.*
2. *If* $|\partial U/\partial y|/(U_f/h)$ *is in fuzzy set 2, then* (u'/U_f) *is in fuzzy set 2.*

. . . and so on.

The membership functions for the fuzzy sets used in these rules are shown in Figure 6. These are derived from the probability distributions of the flume velocity data described by Kettle & Beven (2001). The output fuzzy sets from each rule are aggregated using the sum method as described above. There is no need for the final fuzzy set to be defuzzified to a single crisp number as the model takes advantage of the fact that u' may occur over a range of values for a given velocity shear.

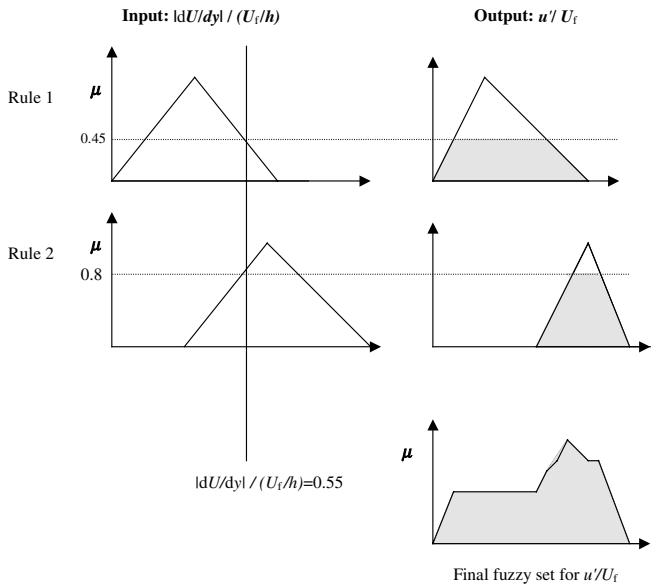

Figure 5 | A simplified example of how a fuzzy inference system uses a value for the non-dimensionalized transverse velocity shear in 2 rules to produce 2 fuzzy sets for the non-dimensionalized velocity fluctuation which are then aggregated to produce a single fuzzy set.

Numerical model

Figure 4 shows that for a significant period of time during the experiment the concentrations changed little over time. It is therefore possible to model the main characteristics of the system as a steady-state simulation. The model is run on a two-dimensional non-orthogonal depth-averaged grid. Telemac 2D is used to generate the mean mass fluxes through each cell face. The mean velocities are derived from these fluxes and input to the fuzzy inference system. The fuzzy inference system then provides the fuzzy set of the fluctuating velocity u' at the cell face. The calculation of the turbulent mass fluxes across each cell face relies on the assumption that each cell is well mixed. The mass fluxes from the mean and fluctuating fields are then used to calculate the transport of mass through the domain.

In the finite-volume formulation, as shown in Figure 7, the diffusive component is conceptualized as an equal and opposite exchange of fluid across a cell boundary. For example, fluid from cell P will move out of the cell at a speed u'_e into cell E, and fluid from cell E will move into cell P at a speed u'_e. Upper-case subscripts denote node points (cell centres) and lower-case subscripts denote cell face values. Integrating over the control volume in Figure 7, with the transported scalar φ_i considered to be constant over the cell face i, and the flow into the cell taken as positive, gives

$$\begin{aligned}&\varphi_w A_w U_w - \varphi_e A_e U_e + \varphi_s A_s V_s - \varphi_n A_n V_n \\ &= u'_w A_w(\varphi_P - \varphi_W) + u'_e A_e(\varphi_p - \varphi_E) \\ &+ v'_s A_s(\varphi_P - \varphi_S) + v'_n A_n(\varphi_P - \varphi_N) \qquad (1)\end{aligned}$$

where A_i is the area of the cell face i given by the product of the depth at location $i(d_i)$ and the length of the cell side

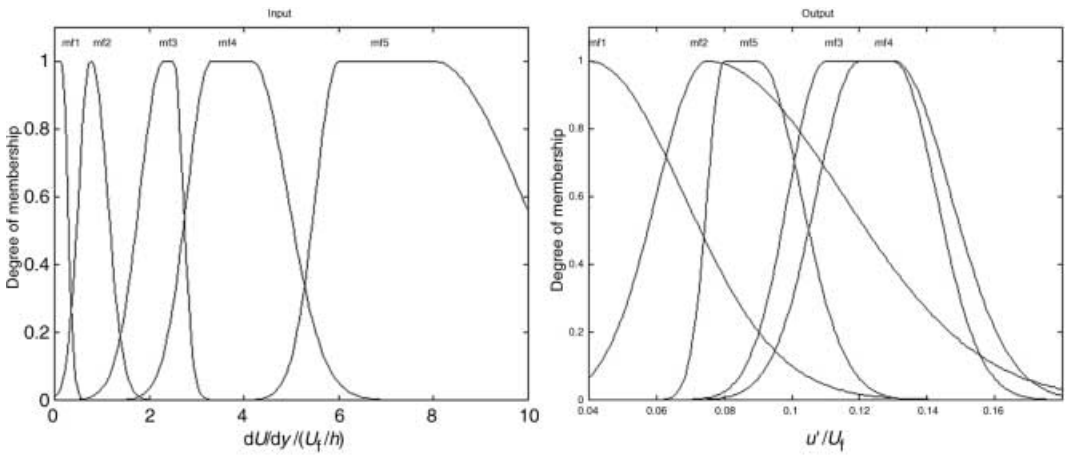

Figure 6 | Input and output membership functions for fuzzy rules relating non-dimensionalized longitudinal velocity fluctuations and transverse velocity shear.

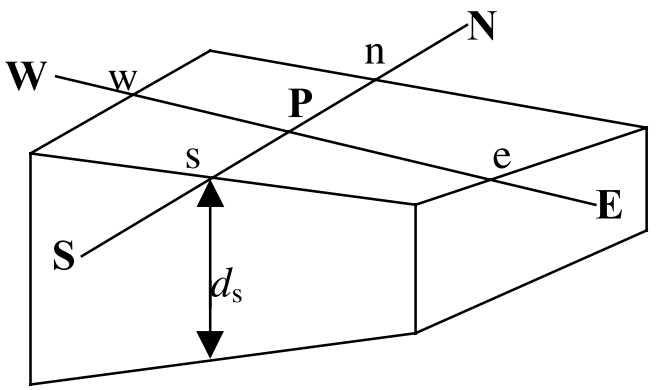

Figure 7 | A control volume around node P.

i, for i = e,w,n,s. This is the general equation for the numerical scheme, which is automatically cast in a fully conservative manner because of the finite-volume formulation.

Hybrid finite-volume scheme

The values of φ at the cell faces in Equation (1) are calculated according to the hybrid scheme (Spalding 1972). This scheme uses a combination of the up-wind and central differencing schemes, such that it exploits the transportiveness of the up-wind scheme and the increased accuracy of central differencing. If the central-difference scheme is used to find the values of φ at the cell faces, then the discretization scheme is only stable and accurate if the ratio of advection to diffusion is less than two. In the work presented here, this non-dimensional value is given by $|U/u'|$, and is equivalent to the Peclet number used in traditional finite-volume schemes, which is defined as $\mathrm{Pe} = |U\Delta x/e_t|$ where Δx is the cell length and e_t is the turbulent diffusion coefficient. Therefore, the hybrid scheme utilizes the central difference scheme to calculate φ at the cell face if $|\mathrm{Pe_T}| < 2$ at that face (where $\mathrm{Pe_T} = U/u'$), otherwise the up-wind scheme is employed. For example, if the east cell face has $|\mathrm{Pe_T}| < 2$, the hybrid scheme uses a central-difference approximation to estimate φ at the east cell face, so that

φ_e = linear interpolation between φ_P and φ_E

However, if the east cell face has $|\mathrm{Pe_T}| \geq 2$, then the up-wind scheme is used, so that

$\varphi_e = \varphi_P$ if $Ue > 0$

$\varphi_e = \varphi_E$ if $U_e < 0$

This is easily applied in two dimensions by treating each cell boundary in the way described above. Once the values of φ at the cell faces have been found in terms of the cell centre values of φ, Equation (1) is rearranged in the form

$$a_p\varphi_P = a_W\varphi_W + a_E\varphi_E + a_S\varphi_S + a_N\varphi_N + S_u \quad (2)$$

with

$$a_P = a_W + a_E + a_N + a_S + (U_e - U_w) + (U_n - U_s) - S_p$$

where the coefficients a_E, a_w, a_N, a_S and a_P depend upon the magnitude of the Peclet number at faces e, w, n and s, and the source term is a function of the dependent variable, such that the source over the cell volume is given by $(S_u + S_p\varphi_P)$. The source term is defined in this way so that it is possible to set the variable φ at node P to a value φ_{fix} by assigning S_p a very large arbitrary value Z and setting S_u to $Z\varphi_{fix}$. The value of Z must be large enough to render the other terms on the right-hand side of Equation (2) negligible, so that $\varphi_P = \varphi_{fix}$ (Versteeg & Malalasekera 1995).

Velocity fluctuations

The mean velocity field produced by Telemac 2D is used to calculate the transverse velocity shear, which is the input to the fuzzy rule system. The rules then produce a fuzzy number for u'. A single value for u' is generated based on the single-value simulation method of fuzzy variables (Dou *et al.* 1997), termed the fuzzy-numerical simulation method by Chanas & Nowakowski (1988). This is done by randomly generating a value t of the membership function on the interval [0,1]. This is the membership value at which the fuzzy set for u' is bounded below so that a new

fuzzy set (known as the t-level set) is created in which each member, u_t', has a membership value greater than t. A value from the t-level set is then randomly chosen to be the single value for u'. The fuzzy number for v' is then found from a fuzzy regression relationship (Bardossy *et al.* 1990) given by

$$v' = 0.7864u' + 0.0038,\ \mu = 1 \tag{3}$$

$$v'^{+} = 1.1664u' + 0.0038,\ \mu = 0$$

$$v'^{-} = 0.4064u' + 0.0038,\ \mu = 0$$

where μ is the membership value of the fuzzy set, and v'^{+} and v'^{-} are the upper and lower velocity bounds. This relationship is derived from laboratory flume data and is given in detail in Kettle & Beven (2001). A single value for v' is then found in a similar way so that the same value of t is used to create the t-level set for v', and then a value from v_t' is chosen at random. The single values of u' and v' are then used in the finite volume to calculate the diffusion. The resulting concentration field gives the distribution for the chosen t-level. Multiple runs give possible concentration fields for each t-level, from which a final fuzzy number for concentration may be reconstructed for each cell.

Figure 8 shows the output for u' from the fuzzy rules when the distribution has been defuzzified to a crisp number by taking the centroid of the fuzzy set. This figure shows that the fuzzy rules predict that the main areas of turbulent activity are concentrated along the bank regions and in the shear zone. This pattern is supported by general observations in the field, but the actual values of the turbulent fluctuations are approximately half the size of those at the corresponding points measured in the flow. This is because the field measurements include large temporal variations in velocity due to the periodic nature of the dead-zone flow system that cannot be accounted for in the steady state. Since the fuzzy rules are derived from velocity measurements taken around a dead zone in a laboratory flume, these oscillations should be inherent in the data used to derive the rules. However, the laboratory dead zone is of length 30 cm and the river dead zone is approximately 100 m in length, so the underestimation of the turbulent fluctuations may reflect a scale problem. It could be that the periodic oscillation of the shear zone is more significant at this much larger scale.

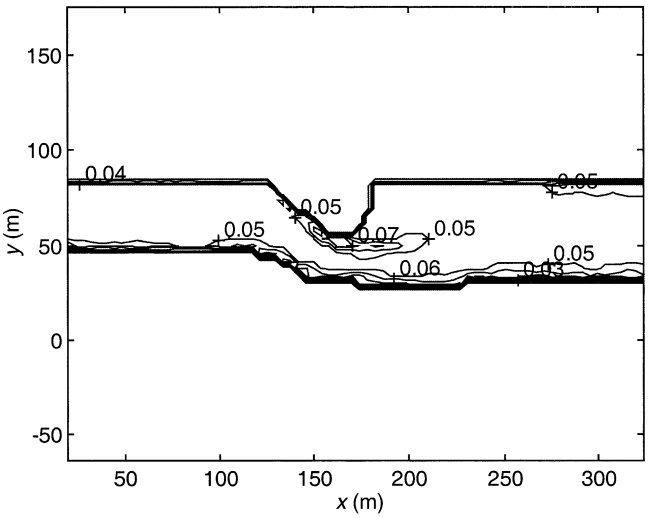

Figure 8 | Longitudinal velocity fluctuations, u', in cm/s taken from the centroid of the fuzzy set produced by the input of $|\partial U/\partial y| / (U_f/h)$ into the fuzzy inference system.

Dye source

In order to simulate the steady-state portion of the experiment accurately, the tracer concentration in the injection site cell is calculated by a mass balance equation and fixed at this value for the simulation. This is done by setting the source terms in this cell as

$$S_u = 10^{30}\varphi_{fix} \text{ and } S_p = -10^{30}$$

When this source is added to the discretized equation it gives

$$(a_P + 10^{30})\varphi_P = \Sigma a_i\varphi_i + 10^{30}\varphi_{fix} \tag{4}$$

The actual value of the number 10^{30} is arbitrary, as it just has to be very large compared with the coefficients a_i. Thus, if the a_i values are negligible in Equation (4), then

$$\varphi_P = \varphi_{fix}$$

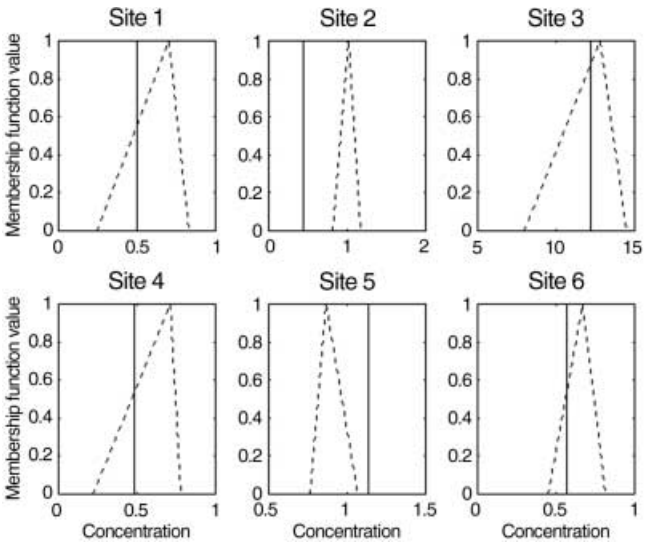

Figure 9 | Steady state concentration (in units of 10^6 kg/m^3) at each sample site. The predicted fuzzy number for concentration is shown by the dotted lines such that the most likely concentration corresponds to a membership value of 1, but all concentrations with membership values greater than zero are possible to lesser extents. The observed data is a single value depicted by a solid line.

Once the coefficient for each node in the domain has been calculated, a large system of linear equations in the form of Equation (2) is obtained. Since there is an equation for each node, solving these equations simultaneously yields the value of φ at each node. These discretized equations are solved using the iterative tri-diagonal matrix algorithm (TDMA) developed by Thomas (1949). It is applied here in an iterative fashion, as described in Versteeg & Malalasekera (1995).

RESULTS AND DISCUSSION

Figure 9 shows that the concentration distribution predicted by the model captures the observed data at the reattachment zone (Site 1), at the start of the shear zone (Site 3), on the dead-zone side of the shear zone (Site 4) and in the centre of the dead zone (Site 6). The concentration at Site 5, which is on the main-flow side of the shear zone, is underestimated, which could be due to the absence of the vertical dimension. The model assumes complete vertical mixing, but over this short distance it is unlikely that the tracer will have mixed through the whole depth in the main flow. Thus, in reality the measured concentration will exceed that predicted by the model. The concentrations at the other sites in the dead zone are generally overestimated, which implies that the model is over-predicting the amount of tracer entering the dead zone. This could be due to an inaccurate mean velocity field or an overestimation of the turbulent mixing laterally across the shear zone. However, given that the turbulent diffusion of the dye is based on fuzzy rules derived from velocity measurements taken from a laboratory flume that is two orders of magnitude smaller than the river dead zone, the fuzzy model produces reasonable results. The periodicity in the river dead zone presents problems when studying the magnitude of the velocity fluctuations, which suggests that a better result could be obtained using the fuzzy rules in a time-dependent flow model.

CONCLUSION

In this paper, an alternative approach to the popular CFD packages based on fuzzy rules has been presented to describe the imprecise nature of mixing in a river situation, and to incorporate this uncertainty into a model structure. The results show that despite the simplification of a time-dependent flow in a complex three-dimensional geometry to a depth-averaged, steady-state situation, it is still possible to predict concentration fields, within degrees of uncertainty, using the fuzzy model. The fuzzy rules also appear to work (to a certain extent) on a variety of scales, from a laboratory flume (Kettle & Beven 2001) to a large river. The flexibility and simplicity of the fuzzy rules allow more information on the flow to be added with ease. Future work may lead to the development of rules relating local bed roughness to turbulent fluctuations. To conclude, fuzzy rules allow non-linear information to be incorporated easily into a finite-volume model so that limiting assumptions about the turbulent field need not be made. This extra information allows the uncertainties inherent in the turbulent field to be carried through the model to produce a distribution of possible concentrations that compare well with those measured in the field.

ACKNOWLEDGEMENTS

Michael Holland, Peter Goldsack, and David Aspinall are thanked for their participation in the field experiment.

NOMENCLATURE

A_e	area of east face (m^2)
a_E	coefficients of φ_E
a_N	coefficients of φ_N
a_P	coefficients of φ_P
a_S	coefficients of φ_S
a_W	coefficients of φ_W
e_t	diffusion coefficient ($m^2\ s^{-1}$)
e	east cell face
h	water depth (m)
μ_A	membership function of fuzzy set A
n	north cell face
P	centre cell node
Pe_T	Peclet number used in model
Pe	Traditional Peclet number
φ	value of property per unit mass
S_p	source term
S_u	source term
s	south cell face
t	time (s)
u'	root mean square of the temporal fluctuating longitudinal velocity ($m\ s^{-1}$)
U	mean longitudinal velocity at a point in the flow domain ($m\ s^{-1}$)
U_f	average longitudinal velocity for all the main flow ($m\ s^{-1}$)
v'	root mean square of the temporal cross-stream fluctuating velocity ($m\ s^{-1}$)
V	mean cross-stream velocity ($m\ s^{-1}$)
W	mean vertical velocity ($m\ s^{-1}$)
w'	root mean square of the temporal vertical fluctuating velocity ($m\ s^{-1}$)
w	west cell face
x	distance (m)

REFERENCES

Bardossy, A. & Duckstein, L. 1995 *Fuzzy Rule-Based Modelling with Applications to Geophysical, Biological and Engineering Systems*. CRC Press, Boca-Raton, FL.

Bardossy, A., Bogardi, I. & Duckstein, L. 1990 Fuzzy regression in hydrology. *Wat. Resour. Res.* **26**, 1497–1508.

Chanas, S. & Nowakowski, M. 1988 Single-value simulation of fuzzy variables. *Fuzzy Sets Syst.* **25**, 43–57.

Dou, C., Woldt, W., Bogardi, I. & Dahab, M. 1997 Numerical solute transport simulation using fuzzy sets approach. *J. Contam. Hydrol.* **27**, 107–126.

Dubois, D. & Prade, H. 1991 Fuzzy sets in approximate reasoning (Parts 1 and 2). *Fuzzy Sets Syst.* **40**, 143–244.

Hankin, B., Hardy, R., Kettle, H. & Beven, K. 2001 Using CFD in a GLUE framework to model the flow and dispersion characteristics of a natural fluvial dead zone. *Earth Surf. Process. Landforms* **26**, 667–687.

Kettle, H. & Beven, K. 2001 Fuzzy rule-based model for solute dispersion in an open-channel dead zone. *J. Hydroinformatics* **4**(1), 39–51.

Lane, S. N., Biron, P. M., Bradbrook, K. F., Butler, J. B., Chandler, J. H., Crowell, M. D., McLelland, S. J., Richards, K. S. & Roy, A. G. 1998 Integrated three-dimensional measurement of river channel topography and flow processes using acoustic Doppler velocimetry. *Earth Surf. Process. Landforms* **23**(13), 1247–1267.

Spalding, D. B. 1972 A novel finite-difference formulation for differential expressions involving both first and second derivatives. *Int. J. Numer. Methods Eng.* **4**, 551–559.

Taylor, G. I. 1921 Diffusion by continuous movements. *Proc. Math. Soc., Ser. 2.* **20**, 196–212.

Thomas, L. H. 1949 Elliptic problems in linear difference equations over a network. Watson Science Computing Laboratory Report, Columbia University, New York.

Versteeg, H. K. & Malalasekera, W. 1995 *An Introduction to Computational Fluid Dynamics: The Finite-Volume Method*. Longman Essex, UK.

Young, P. C. & Wallis, S. G. 1993 Solute transport and dispersion in stream channels. In *Channel Network Hydrology* (eds. Beven, K. A. & Kirby, M. J.). Wiley, Chichester.